Robust TOA-based Navigation under Measurement Model Mismatch in Harsh Propagation Environments

Gaël Pagès and Jordi Vilà-Valls

***Abstract*— Global Navigation Satellite Systems (GNSS) is the positioning technology of choice outdoors but it has many limitations to be used in safety-critical applications such Intelligent Transportation Systems (ITS). Namely, its performance clearly degrades in harsh propagation conditions, these systems are not reliable due to possible attacks, may not be available in GNSS-denied environments, and using standard architectures do not provide the precision needed in ITS. Among the different alternatives, Ultra-WideBand (UWB) ranging is a promising solution to achieve high positioning accuracy. The key points impacting any time-of-arrival (TOA) based navigation system are i) transmitters' geometry, and ii) a perfectly known transmitters' position. In this contribution we further analyze the performance loss of TOA-based navigation systems in real-life applications where we may have both transmitters' position mismatch and harsh propagation conditions, i.e., measurements corrupted by outliers. In addition, we propose a new robust filtering method able to cope with both effects. Illustrative simulation results are provided to support the discussion and show the performance improvement brought by the new methodology with respect to the state-of-the-art.**

I. Introduction

Reliable and precise position, navigation and timing (PNT) information is fundamental in safety-critical applications such as Intelligent Transportation Systems (ITS), automated aircraft landing or autonomous unmanned ground/air vehicles (robots/drones), to name a few. In addition, in the context of ITS, this is not only of capital importance for the autonomously navigating system but also for vulnerable road users such as cyclists and pedestrians, and systems collaterally using this information, i.e., in traffic control and for emergency services. Even if the main source of positioning information are still Global Navigation Satellite Systems (GNSS), they lack of reliability and accuracy in constrained environments such as highly populated areas, which limit their adoption as standalone PNT system. For instance, GNSS may be affected by attacks such as jamming and spoofing [1], or be severely affected in harsh propagation conditions [2]. Moreover, standard GNSS may not provide the precision needed in the ITS context, i.e., sub-meter lane-level. Several GNSS carrier phase-based precise PNT solutions exist to improve the latter, for instance, Real-Time Kinematics (RTK) [3, Ch. 26] or Precise Point Positioning (PPP) techniques [3, Ch. 25], but they need either a reference station or real-time precise corrections, and are even more affected by harsh propagation conditions than standard GNSS code-based techniques. In addition, these systems may not be available at all in the so-called GNSS-denied environments.

Several alternatives to GNSS exist, ranging from the exploitation of cellular signals (LTE/5G) or other signals-of-opportunity, the combination with local inertial navigation systems (INS) or the use of vehicle-to-everything (V2X) communications to obtain peer-to-peer measurements. A different approach is to consider dedicated infrastructure, specifically designed to provide precise ranging measurements. This is the case of Ultra-WideBand (UWB) technologies, which is exploited in this contribution. They are typically based on time-of-arrival (TOA) two-way ranging measurements and can achieve a sub-decimeter level ranging accuracy in line-of-sight (LOS) nominal conditions [4]–[8]. With respect to other ranging technologies, UWB has the additional advantage to be more robust to interferences.

In general, UWB-based navigation has the fundamental drawback that anchor nodes (transmitters) position is assumed to be perfectly known, which may not be the case in real-life applications. Given the sub-decimeter nominal accuracy of the system, this may have a strong impact on the final performance as it has been recently shown in [9]. This is also a critical point if UWB ranging measurements are used in multi-sensor data fusion platforms, for instance in combination with GNSS, which require a common navigation coordinate frame [10]. Therefore, in real-life applications, a mismatch on the transmitters' position is a key point to be carefully analyzed for reliable UWB-based navigation.

In this contribution, based on the preliminary results in [9] where we proposed an augmented state extended Kalman filter (EKF) to cope with possible anchor position mismatch under nominal Gaussian conditions, we further explore UWB-based navigation in realistic scenarios. We consider that several transmitter to receiver links may be affected by multipath or non-line-of-sight (NLOS) conditions, then assuming the typical contamination model arising in robust statistics [11] for certain ranging measurements. Without model mismatch, the standard solution is to consider a robust regression-based EKF, but this methodology does not apply when both outliers and model mismatch are present, mainly because the filter is not able to distinguish between true measurement outliers and measurements which deviate from the nominal due to the mismatch. Instead, we propose to use a robust weighting function as uncertainty indicator within the augmented state EKF, which is used to adapt the measurement noise covariance matrix. Illustrative simulation results are provided to support the discussion ans show the performance improvement brought by the new methodology.

This work has been supported by the DGA/AID projects 2018.60.0072.00.470.75.01 and 2019.65.0068.00.470.75.01.

Authors are with ISAE-SUPAERO, University of Toulouse, Toulouse, France. {name.surname}@isae-supaero.fr

II. Problem Formulation

Consider the positioning of a mobile agent, where at time t both position and velocity are to be inferred, $\mathbf{p}_{m,t} = [x_{m,t}, y_{m,t}, z_{m,t}]^T$ and $\mathbf{v}_{m,t} = [v_{x,t}, v_{y,t}, v_{z,t}]^T$. If L transmitters (Tx) (i.e., anchor nodes or cellular base stations), within the communication range of the target, are located at fixed positions $\mathbf{p}_i = [x_i, y_i, z_i]^T$, with $i = 1, \ldots, L$, then the measured Tx to agent distance is given by :

$$z_{i,t} = ||\mathbf{p}_{m,t} - \mathbf{p}_i|| + n_{i,t}, \tag{1}$$

where $||\cdot||$ is the $L2$-norm,

$$\begin{aligned} d_{i,t} &= ||\mathbf{p}_{m,t} - \mathbf{p}_i|| \\ &= \sqrt{(x_{m,t} - x_i)^2 + (y_{m,t} - y_i)^2 + (z_{m,t} - z_i)^2}, \end{aligned}$$

and n_i a measurement noise. The full set of available observations (measurement equation) is written as:

$$\underbrace{\begin{bmatrix} z_{1,t} \\ \vdots \\ z_{L,t} \end{bmatrix}}_{\mathbf{z}_t} = \underbrace{\begin{bmatrix} ||\mathbf{p}_{m,t} - \mathbf{p}_1|| \\ \vdots \\ ||\mathbf{p}_{m,t} - \mathbf{p}_L|| \end{bmatrix}}_{\mathbf{h}_t(\mathbf{x}_t)} + \underbrace{\begin{bmatrix} n_{1,t} \\ \vdots \\ n_{L,t} \end{bmatrix}}_{\mathbf{n}_t}. \tag{2}$$

In real-life application the number of available observations may be time-varying, then the system must be aware that the size of the measurement vector may be changing over time. Regarding the dynamics of the agent, for simplicity we may consider a constant velocity model (process equation),

$$\underbrace{\begin{bmatrix} \mathbf{p}_{m,t} \\ \mathbf{v}_{m,t} \end{bmatrix}}_{\mathbf{x}_t} = \underbrace{\begin{bmatrix} \mathbf{I}_3 & \Delta t \mathbf{I}_3 \\ \mathbf{0}_3 & \mathbf{I}_3 \end{bmatrix}}_{\mathbf{F}} \underbrace{\begin{bmatrix} \mathbf{p}_{m,t-1} \\ \mathbf{v}_{m,t-1} \end{bmatrix}}_{\mathbf{x}_{t-1}} + \underbrace{\begin{bmatrix} \mathbf{0}_3 \\ \mathbf{w}_{v,t-1} \end{bmatrix}}_{\mathbf{w}_{t-1}}, \tag{3}$$

with $\mathbf{w}_{t-1} \sim \mathcal{N}(\mathbf{0}, \mathbf{Q})$. Both (2) and (3) define the *state-space model (SSM) formulation* of the problem. To further introduce the main problem to be considered in this contribution, we define the following nominal and mismatched SSMs, and how to account for non-nominal propagation conditions.

- Nominal SSM: in the nominal case (i.e., what the mobile agent would like) $\mathbf{p}_i$ are the true Tx positions and the measurement noise is zero-mean Gaussian with equal variance (all measurements have the same quality), $\mathbf{n}_t \sim \mathcal{N}(\mathbf{0}_L, \mathbf{R})$, $\mathbf{R} = \sigma_{r,i}^2 \mathbf{I}_L$.
- Mismatched SSM: in real-life applications we may have a partial knowledge or uncertainty in a subset of Tx positions. In this case, the position mismatch on a subset $\mathcal{U}_e$ of $L_e \leq L$ Tx is written as

$$\tilde{\mathbf{p}}_i = \mathbf{p}_i + \Delta\mathbf{p}_i \text{ for } i \in \mathcal{U}_e, \tag{4}$$

with $\Delta\mathbf{p}_i = [\Delta x_i \ \Delta y_i \ \Delta z_i]^T$ the position error on the i-th Tx, which can be viewed as a bias in its position. The mismatched measured distance (for $i \in \mathcal{U}_e$) is

$$\begin{aligned} \tilde{z}_{i,t} &= ||\mathbf{p}_{m,t} - \tilde{\mathbf{p}}_i|| + n_{i,t} \\ &= ||\mathbf{p}_{m,t} - (\mathbf{p}_i + \Delta\mathbf{p}_i)|| + n_{i,t} \\ &= \sqrt{d_{i,t}^2 + \varepsilon_t(\mathbf{p}_{m,t}, \Delta\mathbf{p}_i)} + n_{i,t}, \end{aligned} \tag{5}$$

with $\varepsilon_t(\mathbf{p}_{m,t}, \Delta\mathbf{p}_i) = -2(\mathbf{p}_{m,t} - \mathbf{p}_i)^T \Delta\mathbf{p}_i + \Delta\mathbf{p}_i^T \Delta\mathbf{p}_i$, and $\mathbf{p}_{m,t}$ and $\Delta\mathbf{p}_i$ (or equivalently $\tilde{\mathbf{p}}_i$) being unknown. We have in this case that $\tilde{\mathbf{z}}_t = \tilde{\mathbf{h}}_t(\mathbf{x}_t) + \tilde{\mathbf{n}}_t$, with the new measurements $\tilde{\mathbf{z}}_t^T = [\tilde{z}_{1,t}, \ldots, \tilde{z}_{L_e,t}, z_{L_{e+1},t}, \ldots, z_{L,t}]$ and the corresponding measurement equation

$$\tilde{\mathbf{h}}_t(\tilde{\mathbf{x}}_t) = \begin{bmatrix} ||\mathbf{p}_{m,t} - \tilde{\mathbf{p}}_1|| \\ \vdots \\ ||\mathbf{p}_{m,t} - \tilde{\mathbf{p}}_{L_e}|| \\ ||\mathbf{p}_{m,t} - \mathbf{p}_{L_e+1}|| \\ \vdots \\ ||\mathbf{p}_{m,t} - \mathbf{p}_L|| \end{bmatrix}, \tag{6}$$

where $\tilde{\mathbf{x}}_t$ can be the original one in (3) or an augmented state (see next Section III-B).

- Harsh propagation conditions: it is known that, for instance in urban environments or indoors, there are several propagation effects which deviate from Gaussianity, then being crucial to design robust methods in order to obtain a reliable solutions. A possible way to account for these conditions is to consider non-Gaussian measurement noise distributions, i.e., Student t, Laplace or skew t [12], [13]. Another approach is to consider the typical contamination model arising in robust statistics [2], [11]: consider a proportion $1 - \varepsilon$ of observations under nominal Gaussian noise, and another proportion $0 \leq \varepsilon \leq 1$ of observations contaminated by an unknown distribution,

$$n_{i,t} \sim (1 - \varepsilon)\mathcal{N}(0, \sigma_{r,i}^2) + \varepsilon\mathcal{H}, \tag{7}$$

where $\mathcal{H}$ is an arbitrary contaminating distribution accounting for possible outliers (i.e., corrupted observations), for instance, a non-zero mean Gaussian distribution with $\sigma_H \gg \sigma_{r,i}$.

The main question is: *how do we estimate the agent's position and velocity under both Tx position mismatch and non-nominal propagation conditions?*

III. Reference EKF-based Solutions

A. Standard Extended KF Solution

Considering the SSM in (2) and (3), it is easy to design an EKF [14], which needs a linearized (approximated) measurement equation, given by the following Jacobian matrix (evaluated at a given point $\mathbf{x}^0$ and with $\mathbf{u}_{i,t} = ||\mathbf{p}^0 - \mathbf{p}_i||$),

$$\mathbf{H}_t = \left.\frac{\partial \mathbf{h}_t(\mathbf{x}_t)}{\partial \mathbf{x}_t}\right|_{\mathbf{x}^0} = \begin{bmatrix} \frac{x^0 - x_1}{\mathbf{u}_{1,t}} & \frac{y^0 - y_1}{\mathbf{u}_{1,t}} & \frac{z^0 - z_1}{\mathbf{u}_{1,t}} & \mathbf{0}_3^T \\ \vdots & \vdots & \vdots & \vdots \\ \frac{x^0 - x_L}{\mathbf{u}_{L,t}} & \frac{y^0 - y_L}{\mathbf{u}_{L,t}} & \frac{z^0 - z_L}{\mathbf{u}_{L,t}} & \mathbf{0}_3^T \end{bmatrix}. \tag{8}$$

The standard TOA-based navigation is obtained by applying the EKF to the assumed model (2)-(3):

$$\begin{aligned} \hat{\mathbf{x}}_{t|t-1} &= \mathbf{F}\hat{\mathbf{x}}_{t-1|t-1} \\ \mathbf{\Sigma}_{x,t|t-1} &= \mathbf{F}\mathbf{\Sigma}_{x,t-1|t-1}\mathbf{F} + \mathbf{Q} \\ \mathbf{K}_t &= \mathbf{\Sigma}_{x,t|t-1}\mathbf{H}_t^T(\mathbf{H}_t\mathbf{\Sigma}_{x,t|t-1}\mathbf{H}_t^T + \mathbf{R})^{-1} \\ \hat{\mathbf{x}}_{t|t} &= \hat{\mathbf{x}}_{t|t-1} + \mathbf{K}_t(\mathbf{z}_t - \mathbf{h}_t(\hat{\mathbf{x}}_{t|t-1})) \\ \mathbf{\Sigma}_{x,t|t} &= (\mathbf{I} - \mathbf{K}_t\mathbf{H}_t)\mathbf{\Sigma}_{x,t|t-1} \end{aligned}$$

with $\mathbf{H}_t = \partial \mathbf{h}_t(\mathbf{x}_t)/\partial \mathbf{x}_t|_{\mathbf{x}_t=\hat{\mathbf{x}}_{t|t-1}}$. Notice that the linear KF recursion is only valid ($t \geq 1$) if $\mathbf{\Sigma}_{x,0|0} = \mathbf{C}_{\mathbf{x}_0}$ and $\widehat{\mathbf{x}}_{0|0} = \mathbb{E}[\mathbf{x}_0]$ (mean and covariance of the initial state) [15], which in practice are unknown, then an important point is the filter initialization. A practical solution is to use as initial estimate the linear minimum variance distortionless response (LMVDR) estimator, which coincides with the weighted least squares estimator (WLSE) of $\mathbf{x}_1$, and is given by

$$\widehat{\mathbf{x}}_{1|1} = \mathbf{\Sigma}_{x,1|1}\mathbf{H}_1^T\mathbf{R}^{-1}\mathbf{z}_1,\ \mathbf{\Sigma}_{x,1|1} = \left(\mathbf{H}_1^T\mathbf{R}^{-1}\mathbf{H}_1\right)^{-1}, \quad (9)$$

which in this case, due to the nonlinearity of the measurement equation must be replaced by an iterative WLSE.

In case of model mismatch, this EKF-based solution is blind because it directly uses the assumed (mismatched) measurements $\tilde{d}_{i,t} = ||\mathbf{p}_{m,t} - \tilde{\mathbf{p}}_i||$. This can always be used and provides an acceptable (i.e., depending on the application requirements) solution if $d_{i,t}^2 >> |\varepsilon_t(\mathbf{p}_{m,t}, \Delta\mathbf{p}_i)|$.

B. Augmented State EKF Solution

An alternative to the previous standard EKF which does not take into account the possible model mismatch was recently proposed in [9]. The idea is to consider an augmented state, $\tilde{\mathbf{x}}_t = [\mathbf{p}_{m,t}\ \mathbf{v}_{m,t}\ \mathbf{p}_{1,t}\ \cdots\ \mathbf{p}_{L_e,t}]^T$, that is, to include the (partially) unknown $\mathbf{p}_i$ into the state to be estimated. The process equation in this case is given by

$$\underbrace{\begin{bmatrix} \mathbf{p}_{m,t} \\ \mathbf{v}_{m,t} \\ \mathbf{p}_{1,t} \\ \vdots \\ \mathbf{p}_{L_e,t} \end{bmatrix}}_{\tilde{\mathbf{x}}_t} = \underbrace{\begin{bmatrix} \mathbf{I}_3 & \Delta t\mathbf{I}_3 & & \\ & \mathbf{I}_3 & & \\ & & & \mathbf{I}_{3L_e} \end{bmatrix}}_{\tilde{\mathbf{F}}} \tilde{\mathbf{x}}_{t-1} + \underbrace{\begin{bmatrix} \mathbf{0}_3 \\ \mathbf{w}_{v,t-1} \\ \mathbf{0}_3 \\ \vdots \\ \mathbf{0}_3 \end{bmatrix}}_{\tilde{\mathbf{w}}_{t-1}}, \quad (10)$$

and the measurement equation as in (2). The corresponding Jacobian matrix (dimension $L \times (6 + 3L_e)$) is

$$\tilde{\mathbf{H}}_t\Big|_{\tilde{\mathbf{x}}_t=\tilde{\mathbf{x}}^0} = \left[\begin{array}{cc|ccc} \mathbf{l}_{1,t} & \mathbf{0}_3^T & -\mathbf{l}_{1,t} & & \\ \vdots & \vdots & & \ddots & \\ \mathbf{l}_{L_e,t} & \mathbf{0}_3^T & & & -\mathbf{l}_{L_e,t} \\ \hline \mathbf{l}_{L_e+1,t} & \mathbf{0}_3^T & \mathbf{0}_3^T & \cdots & \mathbf{0}_3^T \\ \vdots & \vdots & \vdots & \ddots & \vdots \\ \mathbf{l}_{L,t} & \mathbf{0}_3^T & \mathbf{0}_3^T & \cdots & \mathbf{0}_3^T \end{array}\right], \quad (11)$$

with $\mathbf{l}_{i,t} = \left[\frac{x-x_i}{||\mathbf{p}-\mathbf{p}_i||}\ \frac{y-y_i}{||\mathbf{p}-\mathbf{p}_i||}\ \frac{z-z_i}{||\mathbf{p}-\mathbf{p}_i||}\right]$ the LOS pointing vector. It has been shown in [9] that this provides much better results than the standard EKF if not all the Tx positions are partially unknown (i.e., $L_e < L$). In order to take into account the Tx position uncertainty, the measurement noise variance of the possible mismatched measurements is set to:

$$[\tilde{\mathbf{R}}]_{i,i} = \sigma_{r,i}^2 + \sigma_{p,i}^2. \quad (12)$$

A possible choice of $\sigma_{p,i}^2$ is to consider a maximum bias, for instance, an uniformly distributed random position bias $\Delta\mathbf{p}_i \in [-\mathbf{b}_i, \mathbf{b}_i]$, with $\mathbf{b}_i^T = [b_{x,i}\ b_{y,i}\ b_{z,i}]$. If the bias is equal on every coordinate, $b_{x,i} = b_{y,i} = b_{z,i} = b_i$, then $\sigma_{p,i}^2 = b_i^2/3$.

IV. Robust Extended Kalman Filter

How to deal with measurements under the contamination model in (7) has been studied for several decades in the field of robust statistics. A recent publication provides an excellent introduction with several applications to practical signal processing problems [11]. In the sequel we give first a brief introduction on the idea behind the most basic robust methods, and then how a robust weighting function can be used to robustify the augmented state EKF of interest.

A. The Idea behind Robust Estimation

We consider as an example the *linear regression problem*, $\mathbf{y} = \mathbf{H}\mathbf{x} + \mathbf{n}$, where we want to estimate $\mathbf{x}$ and the noise components are i.i.d. If we define the residuals $\mathbf{r} = \mathbf{y} - \mathbf{H}\mathbf{x}$ the solution is given by the least squares (LS) estimator,

$$\hat{\mathbf{x}}_{\text{LS}} = \arg\min_{\mathbf{x}} ||\mathbf{y} - \mathbf{H}\mathbf{x}||^2 \Rightarrow \arg\min_{\mathbf{x}} \sum_{i=1}^{n} \left(\frac{r_i(\mathbf{x})}{\sigma}\right)^2 \quad (13)$$

where we introduced the normalization of the residuals. Notice that a single outlier can destroy our estimate, then not being a robust solution. Instead of using a quadratic function of the residuals, we can consider a general loss function $\rho(\cdot)$ (and its derivative for the minimization $\psi(x) = \frac{\partial\rho(x)}{\partial x}$) as

$$\hat{\mathbf{x}} = \arg\min_{\mathbf{x}} \sum_{i=1}^{n} \rho\left(\frac{r_i(\mathbf{x})}{\sigma}\right), \quad (14)$$

$$\sum_{i=1}^{n} \psi\left(\frac{r_i(\mathbf{x})}{\sigma}\right) \frac{\partial\left(r_i(\mathbf{x})/\sigma\right)}{\partial\mathbf{x}} = \mathbf{0}, \quad (15)$$

and for instance, $\rho_{\text{LS}}(x) = x^2$ and $\rho_{\ell_1}(x) = |x|$ correspond to the LS and ℓ_1 estimators. The most common $\rho(\cdot)$ is the so-called Huber function

$$\rho(x) = \begin{cases} x^2 & \text{if} \quad |x| \leq a \\ 2a|x| - a^2 & \text{if} \quad |x| > a \end{cases}, \quad (16a)$$

$$\psi(x) = \begin{cases} x & \text{if} \quad |x| \leq a \\ a\ \text{sign}(x) & \text{if} \quad |x| > a \end{cases}, \quad (16b)$$

$$w(x) = \begin{cases} \psi(x)/x, \text{ if } x \neq 0 \\ \psi'(0), \text{ if } x = 0 \end{cases} = \min\left\{1, \frac{a}{|x|}\right\}, \quad (16c)$$

where the value a is chosen to obtain a given efficiency (deviation from the optimal under nominal conditions), for instance, $a = 1.345$ for a 95% efficiency. The idea is that residuals with large errors are downweighted. To solve the problem in (15) we need the residuals standard deviation σ, or a robust estimate of it, for instance the normalized median absolute deviation (MAD), $\hat{\sigma}_M$, defined as

$$\hat{\sigma}_M(\mathbf{x}) = c_m\ \text{Med}(|\mathbf{x} - \text{Med}(\mathbf{x})|), \quad (17)$$

where $\text{Med}(\mathbf{x})$ is the median and c_m a normalizing constant (typically $c_m = 1.4815$). Considering the weight function in (16c) it is easy to see that (15) can be rewritten as

$$\sum_{i=1}^{n} w\left(r_i/\hat{\sigma}_M\right)\ \frac{r_i}{\hat{\sigma}_M}\ \frac{\partial\left(r_i/\hat{\sigma}_M\right)}{\partial\mathbf{x}} = 0, \quad (18)$$

which can be solved by an iterative reweighted LS and is the so-called regression M-estimator.

B. Robust Regression EKF

The robust regression M-estimator introduced in the previous section IV-A can be used within the EKF framework in order to obtain a robust EKF [11]. Notice that the problem of interest is the one where we may have outliers in the observations $\mathbf{z}_t$ and the residuals are related to the innovation sequence $\mathbf{z}_t - \mathbf{h}_t(\hat{\mathbf{x}}_{t|t-1})$. A first approach is to use a robust score function $\psi(\cdot)$ in order to directly downweight the innovation vector, then not modifying the EKF recursion. Another more general approach is to reformulate the EKF as a regression problem and then use at every t a robust regression M-estimate of $\mathbf{x}_t$. Refer to [11, Chap. 7] for details. Notice that both approaches were not developed to cope with a possible model mismatch and they are not directly suited for the navigation problem in this contribution. The underlying problem to apply these techniques to the mismatched SSM is that the filter is not be able to distinguish between true measurement outliers and measurements which deviate from the nominal due to the mismatch.

C. Robust Weighting Uncertainty Indicator for Robust EKF

An alternative to the robust regression EKF is to use the robust weighting function in order to update the statistical characteristic of the measurement noise variance. Indeed, the performance of the EKF is highly affected by the measurement covariance matrix, $\mathbf{R}$, therefore one or more contaminated measurements will have a significant impact on the filter performance, i.e., estimated state.

The proposed method is based on the values taken by the normalized residuals (i.e., innovations) as introduced in Section IV-A. In order to reduce the impact of the contaminated measurements on the estimator, the idea is to increase the variance of each contaminated measurement depending on the value of $|r_i/\hat{\sigma}_M|$. To do so, we propose in this study to use the square inverse of Huber's weighting function, as shown in Figure 1, to adjust the measurement noise variances. Thus, in the case of large residuals, i.e. $|r_i/\hat{\sigma}_M| > a$, and in the framework of anchor position mismatch, the variance can be formulated as,

$$[\tilde{\mathbf{R}}]^*_{i,i} = \frac{1}{\left(w\left(r_i/\hat{\sigma}_M\right)\right)^2}\ [\tilde{\mathbf{R}}]_{i,i}. \tag{19}$$

By replacing $w\left(r_i/\hat{\sigma}_M\right)$ by expression (16c), the latter equation can be rewritten as

$$[\tilde{\mathbf{R}}]^*_{i,i} = r_i^2\ \frac{[\tilde{\mathbf{R}}]_{i,i}}{a^2\hat{\sigma}_M^2}. \tag{20}$$

According to this last equation, we note that the variance associated with the contaminated measurement is proportional to squared residual and that it is able to cope with the anchor position mismatch.

V. Illustrative UWB-based Navigation Example

The performance of the proposed robust estimator in Section IV-C, named MRCEKF, is assessed in a simulation environment and compared to the standard EKF (SEKF) in Section III-A, the mismatch EKF (MEKF) in Section III-B, and the robust regression EKF (RREKF) from [11, Chap. 7]. The Huber's score function ($a = 1.345$), as defined in section IV, is used to compute the RREKF and the MRCEKF. The results are obtained from 100 Monte Carlo (MC) runs.

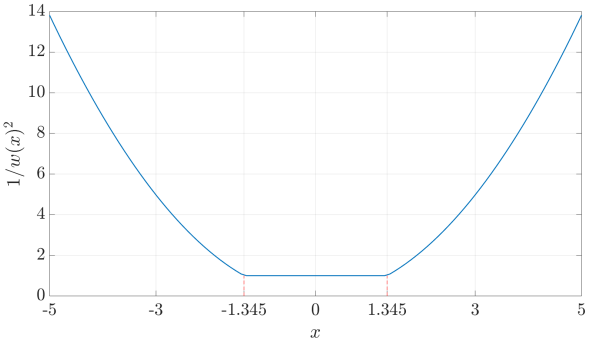

Fig. 1. Square inverse of Huber's weighting function.

A. Simulation Scenario

We consider $L = 8$ anchors and a realistic mobile agent trajectory, shown in Figure 2. The position of five anchors ($A4$ - $A8$) is considered to have a 3-dimensional bias which is drawn randomly in $[-0.5, 0.5]$ m, for each MC run. The unknown state vector to be estimated is then $\mathbf{x}_t = \left[\mathbf{p}_{m,t}, \mathbf{v}_{m,t}, \tilde{\mathbf{p}}_4, \ldots, \tilde{\mathbf{p}}_8\right]^T$.

The initial position and velocity of the agent were set to $\mathbf{p}_{m,0|0} = (0, -2, 0.5)^T$ and $\mathbf{v}_{m,0|0} = (0, 0, 0)^T$ plus a random initial bias of ± 0.5 m and ± 0.01 m.s^{-1}, respectively. The noise of the inlier observations is described by a zero-mean Gaussian distribution whose variance was set to $\sigma^2_{r_i,\text{LOS}} = 0.01$ m^2. Similarly, the NLOS effect (outliers) in the observations is modeled as a zero-mean Gaussian distribution with a variance α^2 times larger than that of the inlier observations. The mixed LOS/NLOS conditions are modeled as a Markovian process that switches between the LOS and NLOS conditions. Different percentages, ε, for the the probability of being in NLOS conditions, and outlier magnitudes, α, are considered and indicated in Table I. The number of anchors in NLOS conditions is drawn randomly within the 8 anchors, and the number of regions and length of each region in mixed LOS/NLOS conditions are also randomly generated.

TABLE I

Parameters for the Monte Carlo simulation.

Number of runs	100
Range variance noise (m^2)	0.01
Number of anchors	8
Number of mismatched anchors	$L_e = 5$
Anchor position bias (cm)	$[-50, +50]$
Outlier percentage ε	$10 - 25 - 50$
Outlier magnitude α	$1 - 5 - 10 - 30 - 60$
Number of NLOS anchors	$2 - 4 - 6 - 8$

B. Results

First, we show in Figure 2 a single realization, and the corresponding four estimates, to clearly illustrate both the

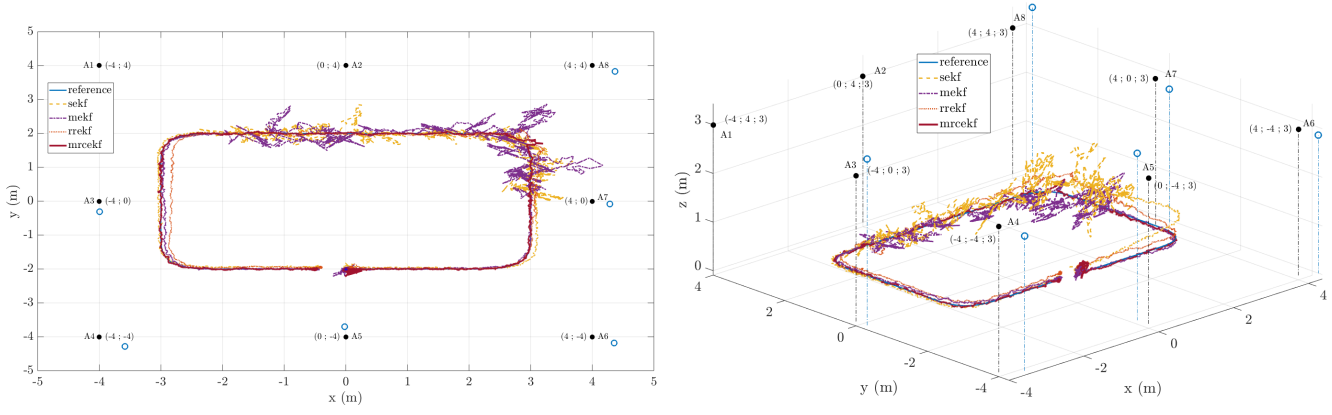

Fig. 2. 2D (left) and 3D (right) trajectories and the corresponding estimates. The scenario is based on 5 anchors out of 8 having a random position bias of ± 0.5m (blue circles). The mixed LOS/NLOS conditions are generated for a specific region of the trajectory and concerns all 8 anchors. They are modeled as a Markovian process with the following parameters: $\sigma_{r_i,\text{NLOS}} = 3$m, $\varepsilon = 25\%$.

impact of the mismatched anchors (blue circles) and harsh propagation conditions (outliers), which are evident in such results. The former can be seen in the 3D plot where the standard SEKF and RREKF are not able to deal with the position mismatch and are affected by a misalignment of the estimated trajectory. Even if the RREKF correctly discards outliers (see 2D plot) it trusts the mismatched anchor positions as being the real ones. The SEKF is not able to cope with neither the mismatch nor outliers. Regarding the augmented state techniques, the MEKF is able to deal with the mismatch but not with the outliers. Notice that only the new MRCEKF provides a smooth trajectory properly dealing with both position mismatch and corrupted measurements.

Figure 3 shows the average horizontal and vertical root mean square errors (RMSE) obtained with the four estimators as a function of the NLOS standard deviation (i.e., $\sigma_{r_i,\text{NLOS}} = \alpha\sigma_{r_i,\text{LOS}}$). We provide the results obtained for 4 and 8 anchors under NLOS conditions, and $\varepsilon = 25$ and 50%. Notice that other configurations were also tested but we only illustrate the most relevant results. As expected, for a given percentage of contamination, the MEKF breaks down rapidly as the amplitude of the outliers increases. Indeed, the MEKF tries to compensate the modeling error due to the mismatch, then measurements corrupted by outliers are understood by the filter as a bias in the anchors' position. In comparison, the SEKF is less affected by this behavior, with no clear performance breakdown, but in general this method provides a worse estimate when compared to the two robust estimators. On the contrary, the RREKF estimator is relatively stable, thus correctly dealing with outliers, but its nominal performance is degraded because of the mismatch.

For low outlier magnitudes, α, it is clear when comparing the outcome of both MEKF and RREKF that a method being able to cope with both mismatch and outliers should retain the best qualities of both estimators. Indeed this is the case with the new MRCEKF which is relatively stable and copes perfectly with contaminated observations and anchor position mismatch, up to a certain level of contamination. This new robust method outperforms the rest when the number of contaminated measurements is less or equal than 6 and $\varepsilon \leq 50\%$. From the results analyzed it can be concluded that for $\varepsilon < 50\%$, $\alpha \leq 3$m and the number of anchors in NLOS conditions ≤ 6, the MRCEKF approach guarantees horizontal and vertical performances below the tens of centimeters, unlike the other approaches.

VI. Conclusion

In this contribution we have shown the impact of both model mismatch (i.e., transmitters' position uncertainty) and harsh propagation conditions (i.e., measurements corrupted by outliers) in realistic UWB-based navigation systems, with a non-negligible performance loss if not properly taken into consideration. A possible way to mitigate both effects is: i) to introduce the uncertain anchors' position into the state to be tracked by a KF-like method, and ii) to resort to robust statistics for the design of robust filtering techniques. We proposed a robust filter able to cope with both model mismatch and corrupted measurements by leveraging a robust weighting function to adapt the measurement noise statistics. This new approach provides a significant performance improvement under several configurations with respect to the state-of-the-art, being a promising solution to be further explored.

References

[1] M. G. Amin, P. Closas, A. Broumandan, and J. L. Volakis, "Vulnerabilities, threats, and authentication in satellite-based navigation systems [scanning the issue]," *Proceedings of the IEEE*, vol. 104, no. 6, pp. 1169–1173, 2016.

[2] D. Medina, H. Li, J. Vilà-Valls, and Pau Closas, "Robust Statistics for GNSS Positioning under Harsh Conditions: a Useful Tool?," *Sensors*, vol. 19, no. 24, Dec. 2019.

[3] P. J. G. Teunissen and O. Montenbruck, Eds., *Handbook of Global Navigation Satellite Systems*, Springer, Switzerland, 2017.

[4] A. R. Jiménez and F. Seco, "Comparing Decawave and Bespoon UWB location systems: Indoor/outdoor performance analysis," in *Proc. of the IEEE International Conference on Indoor Positioning and Indoor Navigation (IPIN)*, Oct. 2016.

[5] J. Tiemann, F. Schweikowski, and C. Wietfeld, "Design of an UWB indoor-positioning system for UAV navigation in GNSS-denied environments," in *Proc. of the IEEE International Conference on Indoor Positioning and Indoor Navigation (IPIN)*, Oct. 2015.

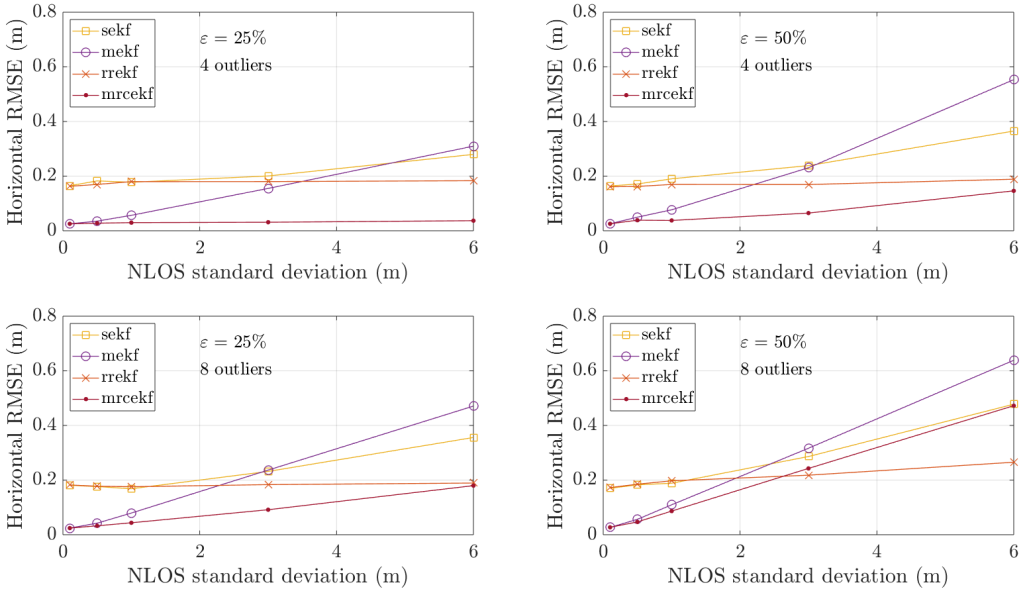

(a)

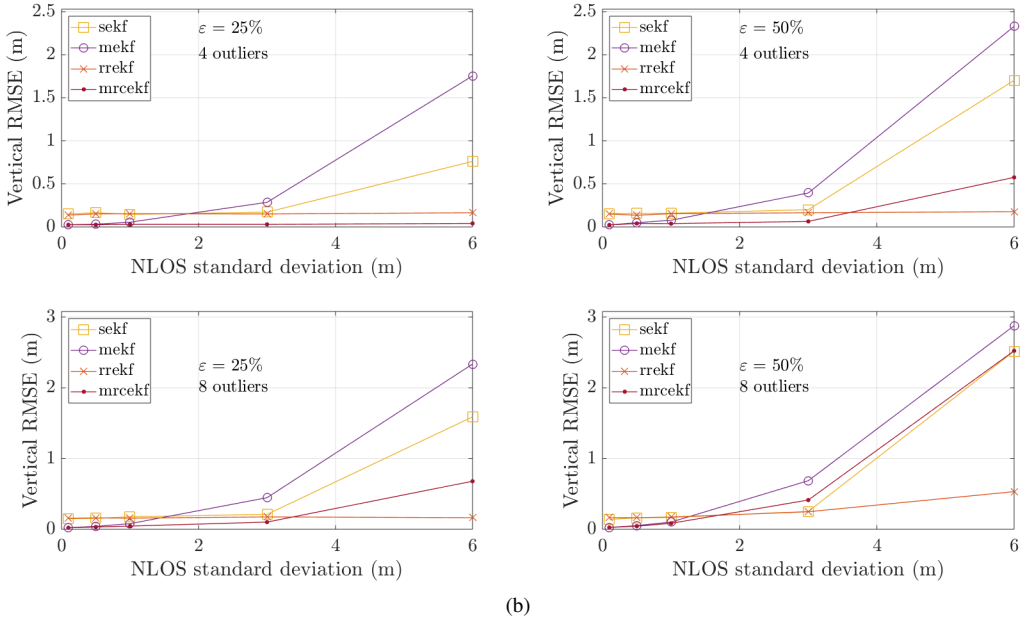

(b)

Fig. 3. Average horizontal (a) and vertical (b) RMSE results for four relevant examples using the standard EKF (SEKF), the mismatch EKF (MEKF), the robust regression EKF (RREKF) and the mismatch robust weight-based EKF (MRCEKF).

[6] J. Tiemann, J. Pillmann, S. Boecker, and C. Wietfeld, "Ultra-wideband aided precision parking for wireless power transfer to electric vehicles in real life scenarios," in *Proc. of the IEEE Vehicular Technology Conference (VTC-Fall)*, Sept. 2016.

[7] M. M. Pietrzyk and T. Von Der Grun, "Experimental validation of a TOA UWB ranging platform with the energy detection receiver," in *Proc. of the IEEE International Conference on Indoor Positioning and Indoor Navigation (IPIN)*, 2010.

[8] O. Cetin et al., "An experimental study of high precision TOA based UWB positioning systems," in *Proc. of the IEEE International Conference on Ultra-Wideband (ICUWB)*, 2012.

[9] G. Pagès and J. Vilà-Valls, "UWB-based Indoor Navigation with Uncertain Anchor Nodes Positioning," in *Proc. of the ION GNSS+*, Miami, FL, USA, Sep. 2019.

[10] Á. Cebrian et al., "Low-Cost Hybrid GNSS/UWB/INS Integration for Seamless Indoor/Outdoor UAV Navigation," in *Proc. of the ION GNSS+*, Miami, FL, USA, Sep. 2019.

[11] A. M. Zoubir, V. Koivunen, E. Ollila, and M. Muma, *Robust Statistics for Signal Processing*, Cambridge Univ. Press, Cambridge, U.K., 2018.

[12] J. Vilà-Valls and Pau Closas, "NLOS Mitigation in Indoor Localization by Marginalized Monte Carlo Gaussian Smoothing," *EURASIP Journal on Advances in Signal Processing*, vol. 62, Aug. 2017.

[13] J. Vilà-Valls, F. Vincent, and Pau Closas, "Decentralized Information Filtering under Skew-Laplace Noise," in *Proc. of Asilomar*, Pacific Grove, CA, USA, Nov. 2019.

[14] B. Anderson and J. B. Moore, *Optimal filtering*, Prentice–Hall, Englewood Cliffs, NJ, 1979.

[15] E. Chaumette et al., "Minimum Variance Distortionless Response Estimators For Linear Discrete State-Space Models," *IEEE Trans. on AC*, vol. 64, no. 2, pp. 2048–2055, 2017.